Comparison of SARS-CoV-2 infection in two non-human primate species: rhesus and cynomolgus macaques

Kinga P. Böszörményi[1], Marieke A. Stammes[2], Zahra C. Fagrouch[1], Gwendoline Kiemenyi-Kayere[1], Henk Niphuis[1], Daniella Mortier[1], Nikki van Driel[3], Ivonne Nieuwenhuis[2], Ella Zuiderwijk-Sick[4], Lisette Meijer[2], Petra Mooij[1], Ed J. Remarque[1], Gerrit Koopman[1], Alexis C. R. Hoste[5], Patricia Sastre[5], Bart L. Haagmans[6], Ronald E. Bontrop[7,8], Jan A.M. Langermans[3,9], Willy M. Bogers[1], Ernst J. Verschoor[1*], and Babs E. Verstrepen[1]

[1]Department of Virology, Biomedical Primate Research Centre (BPRC), Rijswijk, The Netherlands

[2]Department of Parasitology, BPRC, Rijswijk, The Netherlands

[3]Animal Science Department, BPRC, Rijswijk, The Netherlands

[4]Alternatives unit, BPRC, Rijswijk, The Netherlands

[5]Eurofins-Inmunología y Genética Aplicada (Eurofins-INGENASA), Madrid, Spain.

[6]Department of Viroscience, Erasmus University Medical Center, Rotterdam, The Netherlands

[7]Department of Comparative Genetics and Refinement, BPRC, Rijswijk, The Netherlands

[8]Department of Biology, Theoretical Biology and Bioinformatics, Utrecht University, Utrecht, The Netherlands

[9]Department of Population Health Sciences, Unit Animals in Science and Society, Veterinary Faculty, Utrecht University, Utrecht, The Netherlands

24

25 *Corresponding author:

26 E-mail: verschoor@bprc.nl (EV)

27

Abstract

SARS-CoV-2 is a coronavirus that sparked the current COVID-19 pandemic. To stop the shattering effect of COVID-19, effective and safe vaccines, and antiviral therapies are urgently needed. To facilitate the preclinical evaluation of intervention approaches, relevant animal models need to be developed and validated. Rhesus macaques (*Macaca mulatta*) and cynomolgus macaques (*Macaca fascicularis*) are widely used in biomedical research and serve as models for SARS-CoV-2 infection. However, differences in study design make it difficult to compare and understand potential species-related differences. Here, we directly compared the course of SARS-CoV-2 infection in the two genetically closely-related macaque species. After inoculation with a low passage SARS-CoV-2 isolate, clinical, virological, and immunological characteristics were monitored.

Both species showed slightly elevated body temperatures in the first days after exposure while a decrease in physical activity was only observed in the rhesus macaques and not in cynomolgus macaques. The virus was quantified in tracheal, nasal, and anal swabs, and in blood samples by qRT-PCR, and showed high similarity between the two species. Immunoglobulins were detected by various enzyme-linked immunosorbent assays (ELISAs) and showed seroconversion in all animals by day 10 post-infection. The cytokine responses were highly comparable between species and computed tomography (CT) imaging revealed pulmonary lesions in all animals. Consequently, we concluded that both rhesus and cynomolgus macaques represent valid models for evaluation of COVID-19 vaccine and antiviral candidates in a preclinical setting.

Author summary

52 SARS-CoV-2 infection can have a wide range of symptoms. It can cause asymptomatic or mild
53 disease, but can also have a severe, potentially deadly outcome. Vaccines and antivirals will
54 therefore be crucial in fighting the current COVID-19 pandemic. For testing these prophylactic
55 and therapeutic treatments, and investigating the progression of infection and disease
56 development, animal models play an essential role. In this study, we compare the course of
57 SARS-CoV-2 infection in rhesus and cynomolgus macaques. Both species showed moderate
58 disease symptoms as shown by pulmonary lesions by CT imaging. Shedding of infectious virus
59 from the respiratory system was also documented. This study provides a detailed description
60 of the pathogenesis of a low-passage SARS-CoV-2 isolate in two macaque models and suggests
61 that both species represent an equally good model in research for both COVID-19 prophylactic
62 and therapeutic treatments.
63

Introduction

At the end of 2019, the first cases of coronavirus disease 2019 (COVID-19) were described in the Wuhan region, China [1]. Since then, the causative agent of COVID-19, the Severe Acute Respiratory Syndrome Coronavirus 2 (SARS-CoV-2) has spread rapidly across the globe, leading the World Health Organization to officially declare COVID-19 a pandemic on 11 March 2020. To halt the devastating impact of this disease and the ongoing pandemic, vaccines and antiviral therapies are desperately needed, as well as fundamental knowledge to understand the mode of infection and its associated pathologies. Hence, enormous efforts are initiated to develop a wide range of COVID-19 vaccines.

Between humans, transmission mainly occurs via aerosolized droplets after sneezing or coughing or via direct contact with contaminated surfaces. Similar to the related SARS-CoV, SARS-CoV-2 enters the body via docking with its spike (S) protein to the angiotensin-converting enzyme-2 (ACE2) receptor protein [2]. ACE2 is abundantly expressed on cells of the respiratory system but also on a variety of other organ tissues, including those of the brain and the gastrointestinal tract [3]. This wide-spread distribution of the ACE2 receptor may explain the complex clinical picture of COVID-19. The spectrum of COVID-19 ranges from asymptomatic or mild disease, via flu-like illness to a severe, potentially deadly disease [4]. The most typical hallmark of severe COVID-19 is pneumonia leading to respiratory failure, which occurs after the onset of dyspnea and hypoxemia [5]. However, COVID-19 patients may also suffer from a variety of other symptoms, including amongst other gastrointestinal symptoms, neurological disorders, coagulopathy, and cardiac injury [5-8].

Animal models to investigate the progression of infection and disease development, and to evaluate prophylactic and therapeutic treatment options, are essential to warrant progress in SARS-CoV-2 fundamental and applied research. Different animal species have shown their

value in SARS-CoV-2 research. Originally developed to study SARS-CoV [9], transgenic mice that express the ACE2 receptor elucidated various aspects of COVID-19 [10, 11]. Rodent species, such as the Syrian hamster, turned out to be susceptible to infection with SARS-CoV-2, and hamsters were subsequently utilized to test a live-attenuated YF17D-vectored SARS-CoV2 vaccine candidate [12, 13]. Ferrets represent an established animal model to study the pathology and transmission of respiratory viruses, like influenza viruses [14]. During the course of SARS-CoV infection, viral replication was documented in the upper and lower respiratory tract [15]. Transmission of SARS-CoV-2 among ferrets via either air or direct contact has been shown recently, where virus was shed in nasal washes, saliva, feces, and urine of infected animals [16, 17]. Notwithstanding the great importance of rodent and ferret models, also non-human primates (NHPs) will likely play a pivotal role in COVID-19 research. Like with SARS-CoV, NHPs are susceptible to infection with human SARS-CoV-2. Due to their close phylogenetic relationship, NHPs and humans share many immunological and pathological characteristics [18-20]. This makes NHPs suitable for preclinical evaluation of vaccines and antiviral or immunomodulatory compounds to combat SARS-CoV-2. So far, five species of NHPs; rhesus and cynomolgus macaques, common marmosets (C*allithrix jacchus*), African green monkeys (*Chlorocebus sabaeus*), and sacred baboons (*Papio hamadryas*) have featured in SARS-CoV-2 studies. Common marmosets, a small New World monkey species, are susceptible to infection with SARS and MERS coronaviruses [21, 22], but appear to be relatively resistant to infection with SARS-CoV-2 as only low levels of virus replication could be measured [23, 24]. African green monkeys presented robust virus replication and also showed evidence of respiratory disease [25, 26], in contrast to baboons where variable levels of virus replication were measured [24]. The two most widely-used NHP species in biomedical research are rhesus macaques and cynomolgus macaques. Both macaque species had already

proven their value in research on the related coronaviruses that caused the SARS and MERS epidemics [27, 28], and thus are considered relevant NHP models for preclinical COVID-19 studies. Cynomolgus macaques have been deployed in studies describing aspects of SARS-CoV-2 pathogenesis [23, 29, 30], and have been utilized to evaluate the efficacy of hydroxychloroquine as an antiviral compound [31]. Rhesus macaques have also been applied in COVID-19 pathogenesis studies [22, 24, 32, 33], and to test the efficacy of remdesivir in the treatment of SARS-CoV-2 infection [34]. Additionally, several prototype COVID-19 vaccine candidates have received their first efficacy evaluation in the rhesus macaque model [35-42]. Some research groups [23, 24] shed light on the heterogeneity in SARS-CoV-2 infection and investigated disease progression in different NHP species. Most of these studies were conducted by different research teams, and a controlled comparative approach is lacking thus far.

In other NHP disease models, like those developed for AIDS, TB, and influenza research, the choice of macaque (sub)species can influence the disease outcome considerably [43-47]. The choice of a specific NHP species for research on a new and complex disease, like COVID-19, is therefore not a trivial one and the key question which macaque species is best suited to investigate specific aspects of COVID-19 research needs to be answered. To address this issue, we compared SARS-CoV-2 replication in rhesus and cynomolgus macaque species and monitored signs of COVID-19-like disease symptoms for three weeks after infection. The macaques were infected in parallel with the same virus stock, received completely identical treatment, and the course of infection was followed using the same analyses, including monitoring of lung pathology using computed tomography (CT), and continuous telemetric recording of body temperature and activity of the animals.

Results

Infection of macaques with SARS-CoV-2

After administration of the virus in the upper trachea and nose, levels of viral RNA were detectable in the tracheal and nasal swabs of all monkeys at day 1 pi. Viral RNA remained evident in swab samples for several days. In the tracheal swab sample of rhesus macaque R14002, viral RNA was first time below the detection time at 10 days pi. (Fig 1A, S1 Table). The individual variation of SARS-CoV-2 RNA levels detected in the macaques, regardless of species, was considerable. Peak viral RNA levels in the trachea varied between 1.7 x 10^4 copies/ml (R15096; day 1 pi) and 1.8 x 10^8 copies/ml (J16017; day 2 pi). The time frame in which viral genetic material could be detected varied from only one day (R15096; day 1 pi) up to day 10 pi. (animal R14002, RNA in the trachea).

Peak viral loads detected in nasal swabs were generally lower than levels observed in the throat samples and did not exceed 9.5 x 10^4copies/ml (R15090; day 1 pi). The high virus loads measured in the first two days post-infection may suggest that some remaining RNA from the original inoculum was still present. However, in all macaques, viral RNA was also isolated from nasal swabs at later time points, showing that SARS-CoV-2 was excreted via the nose, and thus indicative for viral replication. The total viral RNA production over time is shown in Fig 1B.

The patterns of viral RNA detection in swabs also varied between individuals. The most outstanding observation was made for cynomolgus macaque J16017 that was positive in the nose at day 1 pi, then had no detectable viral RNA for a period of three days, but later the animal became again positive in the nose swabs for three consecutive days. Other animals (R15096, J16004, J16012, and Ji40805) also became PCR-positive again after a period of one or more days characterized by undetectable levels. In the anal swabs, viral genetic material was rarely detected. Only at a few time points, three macaques tested positive, with a

maximum viral RNA load of 3 x 10^3 copies/ml at day 1 pi., namely in cynomolgus macaque J16017. One animal tested positive for viral RNA in blood at a single time point; R15080 at day 5 pi. (S1 Table). Notably, no significant differences in viral RNA loads were calculated between the macaque species (Fig 1B).

Body temperature, activity, clinical symptoms and blood parameters after SARS-CoV-2 infection

Body temperature and activity of each animal was continuously monitored using a Physiotel Digital telemetric device during the entire study. Upon infection, elevated body temperatures were measured in both macaque species, which could be correlated to the episodes of viral replication in the nose and trachea as was evidenced by qRT-PCR. In Fig 2, we show the body temperature alterations from the baseline during the study. In both groups of animals, the body temperature was significantly higher during the first two weeks after infection as compared to later time points (Fig 2). The temperature curves for the individual animals are depicted in the supplementary data (S1 Fig). The group of cynomolgus macaques showed elevated body temperature in the first 8 to 10 days following infection. This is in contrast with the measurements of the rhesus macaques where no substantial rise in temperature was measured, except for two animals (R14002 and R15090) that showed a sudden peak in body temperature of 0.7°C at day 8 pi.

The activity curves measured in the 3-weeks observation period for all individuals are documented in the S2A Fig. The cumulative activity scores in the first 2 weeks pi. were compared with activity scores in the last week of the study period (S2B Fig). The paired t-test illustrated a significantly lower activity in all four rhesus macaques during the first period after

183 infection (p=0.0072), while this difference in cynomolgus macaques was less obvious and only
184 found in 2 out of 4 macaques.
185 We applied a clinical scoring list to enumerate clinical symptoms that may be caused by the
186 SARS-CoV-2 infection (S2 Table). The cumulative clinical scores per week did not exceed 50 (of
187 a maximum 490 score per week; data not shown), confirming the absence of serious COVID-
188 19-related symptoms. However, in the second week of infection, cynomolgus macaques
189 showed more, but still mild, clinical symptoms than rhesus macaques. This was less evident
190 during the first and third weeks, probably due to outlier clinical scores of individual animals
191 (Fig 3).
192 Blood samples were analyzed for changes in cell subsets and in biochemical parameters. These
193 data were related to a set of normal (standard) values derived from uninfected, healthy
194 rhesus, and cynomolgus macaques from the same breeding colony. No significant deviations
195 from the normal values were seen in blood cell subsets of the infected monkeys. C-reactive
196 protein levels, which are increased in COVID-19 patients with pneumonia [48], were not found
197 higher in infected macaques. In humans, acute kidney injury has been related to SARS-CoV-2
198 infection [49, 50], and elevated levels of serum creatinine and blood urea were detected in
199 10-15% of a cohort of COVID-19 patients [51]. Hence, we measured creatinine and urea levels
200 in macaque blood samples at days 0, 5, 10, 14, and 22 pi., but did not find evidence of kidney
201 malfunction in the infected, but otherwise seemingly healthy monkeys. Equally, depending on
202 the severity of the disease, blood coagulation disorders, like highly elevated D-dimer levels,
203 have been reported for patients [52, 53], but no elevated D-dimer levels were measured in
204 either macaque species. Elevated levels of glucose and alanine transferase were measured in
205 the first week pi. in the blood of most animals, and amylase was increased in one rhesus
206 macaque, R15080 (S3 Fig).

207

208 **Detection of lung lesions in macaques after SARS-CoV-2 infection.**

209 Chest CTs of the macaques after infection revealed several manifestations of COVID-19 with
210 a variable time course and lung involvement (Table 1). The most common lesion types that
211 were found in both rhesus and cynomolgus macaques were ground glass opacities (GGO),
212 consolidations, and crazy paving patterns (CCP) (Fig 4).

213 **Table 1. CT scores of lung lesions in SARS-CoV-2-infected macaques**

		Animals							
Days pi		R14002	R15080	R15090	R15096	J16004	J16012	J16017	Ji408005
	0	0	0	0	0	0	0	0	0
	2	0	1	2	2	2	2	0	0
	4	0	0	0	2	0	4	0	0
	6	0	0	0	2	0	5	0	4
	8	3	0	2	3	0	5	3	2
	10	2	2	0	2	2	1	3	4
	12	3	3	0	1	3	1	0	0
	14	1	2	0	3	1	0	0	2
	16	0	0	0	4	3	6	2	4
	22	3	0	0	3	3	6	1	2

214

215 Lung lesions (max. CT score 2/35) were already seen in CTs early after infection on day 2 in 5
216 out of 8 monkeys, three rhesus, and two cynomolgus macaques. Thereafter, lung involvement
217 was seen in most animals and CT scores increased. Around days 8 and 10 pi., lung lesions were
218 manifest in all animals, and in several macaques the coverage had increased (Table 1). Again,
219 individual variations in lung pathology were considerable; for instance, rhesus macaque
220 R15090 showed low CT scores of 2 only at days 2 and 8 pi, while rhesus macaque R15096 had
221 positive CT scores at all time points after experimental infection, varying from 1 to 4.
222 Cynomolgus macaque J16012 suffered from serious lung damage as early as day 4 pi (score 5)
223 and had a positive chest CT at 8 out of 9 time points. In Fig 5, the cumulative CT scores over

the monitoring period are depicted. The increase in cumulative CT score was 0.692 points per day (95% CI 0.657 to 0.726) and no difference was observed between rhesus and cynomolgus macaques (P = 0.2708).

Immune response to SARS-CoV-2 infection

Humoral immune responses developed relatively fast after infection (Fig 6 and S4 Fig). Total immunoglobulin (Ig) in serum was detected by the DR-ELISA. The antibody response directed to the nucleoprotein (N) of SARS-CoV-2 became evident between day 10 and 12 pi., and continued to rise thereafter, but with individual variations in total Ig levels and patterns. While Ig levels in several animals, both rhesus and cynomolgus macaques, continued to rise until day 21 pi., the Ig levels in others already showed first signs of a decline at day 17 pi. The total Ig pattern seen in the sera of all macaques was reflected by the measurement of IgG directed to the N protein in the same sera. Notably, the development of IgM titers was barely detected in the longitudinal serum samples. In sera from only one animal, cynomolgus macaque J106012, IgM was detectable, beginning at day 12 pi. but titers already started to decline to baseline levels at the end of the study at day 22 pi.

Cytokine and chemokine measurements

Serum levels of 13 cytokines and chemokines were measured to examine the nature of the inflammatory response triggered by the infection with SARS-CoV-2. We investigated if any species differences could be distinguished in the inflammatory response to infection. All metadata obtained from the individual animals are depicted in S5 Fig. Directly upon infection, IP-10 and MCP-1 levels peaked in sera of all cynomolgus macaques. The IP-10 peak at day 2 pi. quickly returned to baseline values. In contrast, in rhesus macaques, only a minor rise in

IP-10 levels was observed at the same time interval. In the same time span, but in both macaque species, the levels of chemokine MCP-1 (CCL2) increased. Levels of other chemokines, like eotaxin (CCL11), MIP-1α (CCL3), MIP-1β (CCL4), but also the cytokines IL-6 and IFN-γ dropped in the first week after infection and started rising around two weeks pi. This decline of particular serum cytokine and chemokine levels coincided with the time period that viral RNA was detectable in nasal and tracheal swabs, indicative for virus production. A different pattern was seen for RANTES (CCL5) and TNFα proteins; serum levels were high in the first 2 weeks after infection and then started decreasing to undetectable levels. RANTES serum concentrations also showed an initial drop very early after infection. This was most prominent in the cynomolgus macaques where RANTES levels dropped to zero on day 1 pi. and started to increase at day 6 pi. Post-infection levels of I-TAC (CXCL11), MIG (CXCL9), and IL-8 (CXCL8) were below detection or were not influenced by the SARS-CoV-2 infection.

Discussion

In humans, COVID-19 was initially regarded as a respiratory disease, but now it is clear that individuals that succumb to this disease can display a complex array of pathologies that cover a broad spectrum of symptoms. To sort out the factors leading to the different COVID-19 manifestations, animal models are essential. Due to their similarity to humans, specifically, non-human primates can play a pivotal role in this type of preclinical research. To best appreciate the potential of the various macaque species as SARS-CoV-2 infection models, a thorough characterization of the course of infection is needed. The comparative study reported in this communication contributes to the knowledge, but more importantly validates the macaque models that are currently in use in SARS-CoV-2 research.

Unlike in some human patients, we found no evidence for renal involvement or coagulation disorders in our monkeys. Equally, increasing C-reactive protein (CRP) levels are a marker in the early diagnosis of pneumonia [48], but different from humans; these levels were not subject to change in the infected macaques during the 3-weeks monitoring period. A direct comparison with humans is hampered by the fact that the macaques were infected, but seemingly healthy, while most published findings in humans were obtained from COVID-19 patients in various stages of disease. Unbiased measurement of the body temperature and activity of each animal was done using a telemetric device implanted in the abdomen. Monitoring by telemetry is an important asset as in both macaque species a notable difference in body temperature was recorded in the first 2 weeks (period of active virus replication) as compared to the third week. Significant differences in animal activity indicated that SARS-CoV-2 infection also influenced the well-being of the animals without causing obvious clinical symptoms. Notably, the elevation in body temperature on the first day of infection, as was reported by Munster *et al*., was not seen in our study, possibly pointing to a potential difference in the sampling method. While we used 24/7 monitoring, in the study described by Munster *et al.*, temperature was measured only on selected days on anesthetized animals [54]. However, variation can also be due to a difference between the challenge viruses used, the methods used for virus inoculation, or the origin and adaptation of the animals used.

Antibody responses were detectable in all animals after infection. Interestingly, no IgM was detected in 7 out of 8 animals. This result was confirmed by a second, in-house developed IgM-ELISA, but instead, the SARS-CoV-2 S protein was used as coating antigen. This approach excludes a technical flaw in the serological assay used. We cannot explain the lack of IgM response to infection, but similar observations were made in an infection study using African Green monkeys. Hartman *et al.* did detect IgM, but the titers were very low, not exceeding

295 1Log_{10} above the assay limit of detection [26]. In contrast, the development of IgG accurately
296 followed the course of virus infection, as it became first detectable within one week after the
297 virus had become undetectable in sera by RT-PCR. This was in line with findings of others [25,
298 26, 29].
299 In a subset of COVID-19 patients, the acute respiratory syndrome coincides with a 'cytokine
300 storm' or hypercytokinemia, which eventually can result in multi-organ failure [55]. Patients
301 with severe COVID-19 symptoms on intensive care units had significantly elevated plasma
302 levels of proinflammatory cytokines, like IL-2, IL-7, IL-10, GSCF, IP-10, MCP-1, MIP-1α, and TNF-
303 α [56]. In this study, macaques did not show overt disease symptoms of COVID-19, but certain
304 cytokines, like IL-6, IFN-γ, MIP-1α, and MIP-1β increased in the plasma of both macaque
305 species, indicating the involvement of the chemokine system during SARS-CoV-2 infection.
306 The cytokine profiles after SARS-CoV-2 were highly comparable between species, except for
307 IP-10 and MCP-1, suggesting differential involvement of monocyte activation between the
308 two species. The similarity in cytokine response after SARS-CoV-2 infection contrasts with
309 observations made after infection of macaques with another respiratory virus, pandemic
310 H1N1 influenza [47]. In that study, macaque species-specific cytokine responses (IL-6, MCP-1,
311 IL-15, IL-1Ra, MIP-1α, and IL-8) were induced upon infection with pH1N1, highlighting the virus
312 type-specific reaction of the chemokine system.
313 Unlike most published studies, we decided not to conduct a necropsy on animals early, 4-5
314 days, post-infection. At that time point after infection, evidence was found for acute viral
315 interstitial pneumonia [30, 32, 34, 54]. Instead, we performed CT imaging to visualize lung
316 pathology induced by SARS-CoV-2. In humans, the sensitivity of CT scanning for lung pathology
317 is high (positive predictive value of 92%), but the type of lesions found are not COVID-19-
318 specific, and can also be observed in a number of other infectious and non-infectious diseases

[57, 58]. In this study, we used purpose-bred NHPs with a well-documented health status and we could compare the scans with a CT obtained just before infection. Therefore, CT imaging provides a valuable tool to specifically monitor the progression of COVID-19-related lung pathology during the entire course of the study. Based on the criteria set to determine clinical severity [59], the macaques in our panel featured moderate disease levels as all eight individuals show levels of pneumonia. In another study using only cynomolgus macaques and using CT imaging as well, lesions were found as early as 2 days post-infection in infected animals [29]. Type-wise, the lung lesions described in that report were comparable to the ones in this communication, but they tend to be located deeper in the lungs. An explanation for this difference may be that the method of instillation of the virus is the underlying cause. Finch *et al*. administered the virus into each bronchus by direct bilateral primary post-carinal intrabronchial instillation, whereas we applied the virus relatively high in the trachea, just below the vocal cords. For similar reasons as reported by the same research team [29], we did not collect bronchoalveolar lavage (BAL) samples from our animals to avoid unwanted interventions in the natural infection process caused by SARS-CoV-2. Studies performed at our institute with respiratory viruses have shown that lung lavages can indeed significantly influence the infection process (manuscript in preparation). Instead of BAL samples, we collected tracheal swabs for virological analysis. The viral RNA loads, but also the temporal pattern of detection in swabs samples were like those observed in BAL samples from other studies [22, 24, 34, 38]. This demonstrates that tracheal swabs are a good alternative for BAL sampling. In addition, the collection of tracheal swabs is a less invasive technique that causes relatively minor discomfort to the animals.

In most SARS-CoV-2 studies in non-human primates, the animals are euthanized shortly after infection in the first week, or after a period of 3 weeks. The animals from this study were not

343 euthanized to be able to perform re-infection studies or to monitor them for late clinical signs,
344 or co-morbidities related to COVID-19.
345 We conclude that the course of SARS-CoV-2 infection of both macaque species is highly
346 similar, indicating that they are equally suitable models to test vaccines and antivirals in a
347 preclinical setting for safety and efficacy. The macaque model for SARS-CoV-2 infection in
348 humans manifests important virological aspects of this disease in humans. Given their
349 immunological and physiological resemblance to humans, NHPs likely will continue to play a
350 pivotal role in research for both COVID-19 prophylactic and therapeutic treatments.
351

352 ## Materials and Methods

353 ### Ethics and Biosafety Statement

354 All housing and animal care procedures took place at the Biomedical Primate Research Centre
355 (BPRC) in Rijswijk, the Netherlands. The BPRC is accredited by the American Association for
356 Accreditation of Laboratory Animal Care (AAALAC) International and is compliant with
357 European directive 2010/63/EU as well as the "Standard for Humane Care and Use of
358 Laboratory Animals by Foreign Institutions" provided by the Department of Health and Human
359 Services of the US National Institutes of Health (NIH, identification number A5539-01). Upon
360 positive advice by the independent ethics committee (DEC-BPRC) the competent authorities
361 (CCD, Central Committee for Animal Experiments) issued a project license (license
362 AVD5020020209404). Approval to start was obtained after further assessment of the detailed
363 study protocol by the institutional animal welfare body (AWB) (in Dutch: Instantie voor
364 Dierenwelzijn, IvD). All animal handlings were performed within the Department of Animal
365 Science (ASD) according to Dutch law. ASD is regularly inspected by the responsible national
366 authority (Nederlandse Voedsel- en Warenautoriteit, NVWA), and the AWB.

367

368 **Animals**

369 Four Indian-origin rhesus macaques and four cynomolgus macaques were used in this study
370 (S3 Table). All macaques were mature, outbred animals, purpose-bred, and housed at the
371 BPRC. The animals were in good physical health with normal baseline biochemical and
372 hematological values. All were pair-housed with a socially compatible cage-mate in cages of
373 at least 4 m^3 with bedding to allow foraging and were kept on a 12-hour light/dark cycle. The
374 monkeys were offered a daily diet consisting of monkey food pellets (Ssniff, Soest, Germany)
375 supplemented with vegetables and fruit. Enrichment was provided daily in the form of pieces
376 of wood, mirrors, food puzzles, and a variety of other homemade or commercially available
377 enrichment products. Drinking water was available *ad libitum* via an automatic watering
378 system. Animal Care staff provided daily visual health checks before infection, and twice-daily
379 after infection. The animals were monitored for appetite, general behavior, and stool
380 consistency. All possible precautions were taken to ensure the welfare and to avoid any
381 discomfort to the animals. All experimental interventions (intratracheal and intranasal
382 infection, swabs, blood samplings, and CT scans) were performed under anesthesia.

383

384 **Virus stock**

385 The animals were infected with the SARS-CoV-2 strain BetaCoV/BavPat1/2020. This strain was
386 isolated from a patient who traveled from China to Germany, and an aliquot of a Vero E6 cell
387 culture was made available through the European Virus Archive-Global (EVAg). The viral stock
388 for the infection study was propagated on Vero E6 cells. For this study, a fifth passage virus
389 stock was prepared with a titer of 3.2×10^6 $TCID_{50}$ per ml. The integrity of the virus stock was
390 confirmed by sequence analysis.

391

392 **Experimental infections and post-exposure study follow-up**

393 Three weeks before the experimental infection, a Physiotel Digital device (DSI Implantable
394 Telemetry, Data Sciences International, Harvard Bioscience, UK) was implanted in the
395 abdominal cavity of each animal. This device allowed the continuous real-time measurement
396 of the body temperature and the animals' activity remotely using telemetry throughout the
397 study.

398 At day 0, all animals were exposed to a dose of 1 x 10^6 $TCID_{50}$ of SARS-CoV-2, diluted in 5 ml
399 phosphate buffered saline (PBS). The virus was inoculated via a combination of the
400 intratracheal route (4.5 ml) and intranasal route (0.25 ml per nostril). Virus infection was
401 monitored for 22 days, during which period the animals were checked twice-daily by the
402 animal caretakers and scored for clinical symptoms according to a previously published,
403 adapted scoring system [60] (S2 Table). A numeric score of 35 or more per observation time
404 point was predetermined to serve as an endpoint and justification for euthanasia. Every time
405 an animal was sedated, the body weight was measured. Blood was collected using standard
406 aseptic methods from the femoral vein at regular time points post-infection (pi). In parallel,
407 tracheal, nasal, and anal swabs were collected using Copan FLOQSwabs (MLS, Menen,
408 Belgium). Swabs were placed in 1 ml DMEM, supplemented with 0.5% bovine serum albumin
409 (BSA), fungizone (2.5 µg/ml), penicillin (100 U/ml), and streptomycin (100 µg/ml) and directly
410 transported to the BSL3 lab.

411

412 **Biochemistry and hematology analysis**

413 Clinical biochemistry was performed using a Vetscan VS2 Chemical analyzer (Zoetis Benelux,
414 Capelle aan de IJssel, The Netherlands) with the use of the Comprehensive Diagnostic profile.

This profile allows testing for alanine aminotransferase, albumin, alkaline phosphatase, amylase, calcium, creatinine, globulin, glucose, phosphorus, potassium, sodium, total bilirubin, total protein, and blood urea nitrogen. Hematology was performed using a Vetscan HM5 Hematology analyser (Zoetis Benelux, Capelle aan de IJssel, The Netherlands). C-reactive protein and D-dimer levels were measured using Cobas Integra 400 plus analyzer (Roche Diagnostics Nederland B.V.).

Viral RNA detection

Viral RNA was isolated from plasma and swab sample supernatants using a QIAamp Viral RNA Mini kit (Qiagen Benelux BV, Venlo, The Netherlands) following the manufacturer's instructions. Viral RNA was reverse-transcribed to cDNA using a Transcriptor First Strand cDNA Synthesis kit (Roche Diagnostics BV, Almere, The Netherlands). Viral RNA was quantified by real-time quantitative RT-PCR specific for the RdRp gene of SARS-CoV-2, as described by Corman *et al*. [61]. The lower detection limit of the qRT-PCR was 3.6 viral RNA copies per reaction.

Computed tomography

Computed tomography (CT) data were acquired on several time points until day 22 (D0, 2, 4, 6, 8, 10, 12, 14, 16, 22 post-infection) using a MultiScan Large Field of View Extreme Resolution Research Imager (LFER) 150 PET-CT (Mediso Medical Imaging Systems Ltd., Budapest, Hungary). Animals were sedated with ketamine (10 mg/kg ketamine hydrochloride (Alfasan Nederland BV, Woerden, The Netherlands) combined with medetomidine hydrochloride, 0.05 mg/kg (Sedastart; AST Farma B.V., Oudewater, The Netherlands) to induce sedation and muscle relaxation, both applied intramuscularly (IM). The monkeys were positioned head first

supine (HFS) with the arms up and fixated in a vacuum pillow. A single CT of the thorax takes 35 seconds by which respiratory motion is inevitable, therefore, to mitigate the impact of respiratory motion and improve the image quality, respiratory gating was applied. The respiratory amplitude was detected with a gating pad placed next to the belly button. At the end of the procedure, when the macaques returned to their home cage, atipamezole (Sedastop; AST Farma B.V., Oudewater, The Netherlands) was given IM (0.25 mg/kg).

For the final reconstruction, the expiration phases were exclusively used and manually selected. A semi-quantitative scoring system for chest CT evaluation was used to estimate SARS-CoV-2-induced lung disease [29, 62]. Quantification of the CTs was performed independently by two persons based on the sum of the lobar scores. The degree of involvement in each zone was scored as: 0 for no involvement, 1 for <5%, 2 for 5-24%, 3 for 25-49%, 4 for 50-74% and 5 for >=75% involvement. An additional increase or decrease of 0.5 was used to indicate alterations in CT density of the lesions. By using this scoring system, a maximum score of 35 could be reached for the combined lobes per time point.

Assessment of cytokine and chemokine protein levels in serum

Cytokine and chemokine concentrations in sera of infected macaques, including IL-1β, IL-6, CCL11 (Eotaxin), CXCL10 (IP-10), CXCL11 (I-TAC), CCL2 (MCP-1), CXCL9 (MIG), CCL3 (MIP-1α), CCL4 (MIP-1β), CCL5 (RANTES), CXCL8 (IL-8), TNFα, and IFNγ, were determined using LEGENDplex™ NHP Chemokine/Cytokine Panel (13-plex) (Biolegend, San Diego, CA, USA) according to manufacturer's instruction. Samples were measured on an LSRII FACS machine and analyzed by using company software.

Antibody response

The total antibody response in macaque sera was analyzed in a double recognition enzyme-linked immunosorbent assay (DR-ELISA) that detects total immunoglobulins in serum and targeted to the SARS-CoV-2 nucleoprotein (N) protein as described by Hoste *et al.* [63] (INgezim COVID19 DR; Eurofins-INGENASA, Madrid, Spain). Additionally, two in-house indirect ELISAs were used to detect monkey immunoglobulin G (IgG) and immunoglobulin M (IgM) directed to SARS-CoV-2 N protein. Briefly, Corning® 96-Well High-Binding Flat-Bottom Microplates were coated with N protein and incubated overnight at 4°C in carbonate buffer, pH 9.6. After washing the wells with PBS pH 7.4/0.05% Tween 20 (PBST), a blocking step was performed with StabilZyme® SELECT Stabilizer (SurModics, Inc., Eden Prairie, MN, USA) for 1h at room temperature (RT). The plate was then incubated with serum samples diluted 1:100 in PBST with 2.5% fetal bovine serum (Gibco; Thermo Fisher Scientific, Inc., Waltham, MA, USA) for 1h at RT. Two positive, cut-off, and negative controls were added to each plate. For macaque-IgG detection, the wells were washed as described above and incubated with Peroxidase-conjugated AffiniPure Goat Anti-Human IgG, Fcγ Fragment Specific (Jackson ImmunoResearch Laboratories, Inc., PA, USA) diluted 1:25 000 in StabilZyme® HRP Conjugate Stabilizer (SurModics), supplemented with 0.5M NaCl for 1h at RT. Finally, after a washing step, the plate was incubated for 15 min with the substrate (TMB-MAX, Neogen Corporation, Lexington, KY, USA) and the reaction was stopped by addition of 0.5 M sulfuric acid. The absorbance was measured at 450 nm using a SpectraMax M5 plate reader (Molecular Devices, LLC., San Jose, CA, USA). To detect macaque-IgM, the same protocol was followed, but the secondary antibody used was an anti-Monkey IgM (μ-chain specific)-Peroxidase antibody produced in goat (Sigma-Aldrich, Merck KGaA, MI, USA) at 1:5000 dilution.

Acknowledgements

487 We would like to thank the Animal Science Department, especially the animal caretakes and
488 veterinarians for excellent care of the animals. We also thank Cristina Aira (Eurofins Ingenasa,
489 Madrid) for technical assistance.

490

References:

1. Chan JF, Yuan S, Kok KH, To KK, Chu H, Yang J, et al. A familial cluster of pneumonia associated with the 2019 novel coronavirus indicating person-to-person transmission: a study of a family cluster. Lancet. 2020;395(10223):514-23. Epub 2020/01/28. doi: 10.1016/S0140-6736(20)30154-9. PubMed PMID: 31986261; PubMed Central PMCID: PMCPMC7159286.
2. Hoffmann M, Kleine-Weber H, Schroeder S, Kruger N, Herrler T, Erichsen S, et al. SARS-CoV-2 Cell Entry Depends on ACE2 and TMPRSS2 and Is Blocked by a Clinically Proven Protease Inhibitor. Cell. 2020;181(2):271-80 e8. Epub 2020/03/07. doi: 10.1016/j.cell.2020.02.052. PubMed PMID: 32142651; PubMed Central PMCID: PMCPMC7102627.
3. Hamming I, Timens W, Bulthuis ML, Lely AT, Navis G, van Goor H. Tissue distribution of ACE2 protein, the functional receptor for SARS coronavirus. A first step in understanding SARS pathogenesis. J Pathol. 2004;203(2):631-7. Epub 2004/05/14. doi: 10.1002/path.1570. PubMed PMID: 15141377; PubMed Central PMCID: PMCPMC7167720.
4. Verity R, Okell LC, Dorigatti I, Winskill P, Whittaker C, Imai N, et al. Estimates of the severity of coronavirus disease 2019: a model-based analysis. Lancet Infect Dis. 2020;20(6):669-77. Epub 2020/04/03. doi: 10.1016/S1473-3099(20)30243-7. PubMed PMID: 32240634; PubMed Central PMCID: PMCPMC7158570.
5. Berlin DA, Gulick RM, Martinez FJ. Severe Covid-19. N Engl J Med. 2020. Epub 2020/05/16. doi: 10.1056/NEJMcp2009575. PubMed PMID: 32412710.
6. Han C, Duan C, Zhang S, Spiegel B, Shi H, Wang W, et al. Digestive Symptoms in COVID-19 Patients With Mild Disease Severity: Clinical Presentation, Stool Viral RNA Testing, and Outcomes. Am J Gastroenterol. 2020;115(6):916-23. Epub 2020/04/18. doi: 10.14309/ajg.0000000000000664. PubMed PMID: 32301761; PubMed Central PMCID: PMCPMC7172493.
7. Paterson RW, Brown RL, Benjamin L, Nortley R, Wiethoff S, Bharucha T, et al. The emerging spectrum of COVID-19 neurology: clinical, radiological and laboratory findings. Brain. 2020. Epub 2020/07/09. doi: 10.1093/brain/awaa240. PubMed PMID: 32637987; PubMed Central PMCID: PMCPMC7454352.
8. Puntmann VO, Carerj ML, Wieters I, Fahim M, Arendt C, Hoffmann J, et al. Outcomes of Cardiovascular Magnetic Resonance Imaging in Patients Recently Recovered From Coronavirus Disease 2019 (COVID-19). JAMA Cardiol. 2020. Epub 2020/07/31. doi: 10.1001/jamacardio.2020.3557. PubMed PMID: 32730619; PubMed Central PMCID: PMCPMC7385689.
9. Peiris JS, Lai ST, Poon LL, Guan Y, Yam LY, Lim W, et al. Coronavirus as a possible cause of severe acute respiratory syndrome. Lancet. 2003;361(9366):1319-25. Epub 2003/04/25. doi: 10.1016/s0140-6736(03)13077-2. PubMed PMID: 12711465; PubMed Central PMCID: PMCPMC7112372.
10. McCray PB, Jr., Pewe L, Wohlford-Lenane C, Hickey M, Manzel L, Shi L, et al. Lethal infection of K18-hACE2 mice infected with severe acute respiratory syndrome coronavirus. J Virol. 2007;81(2):813-21. Epub 2006/11/03. doi: 10.1128/JVI.02012-06. PubMed PMID: 17079315; PubMed Central PMCID: PMCPMC1797474.
11. Lutz C, Maher L, Lee C, Kang W. COVID-19 preclinical models: human angiotensin-converting enzyme 2 transgenic mice. Hum Genomics. 2020;14(1):20. Epub 2020/06/06. doi:

10.1186/s40246-020-00272-6. PubMed PMID: 32498696; PubMed Central PMCID: PMCPMC7269898.

12. Sanchez Felipe L, Vercruysse T, Sharma S, Ma J, Lemmens V, van Looveren D, et al. A single-dose live-attenuated YF17D-vectored SARS-CoV2 vaccine candidate. Nature. 2020 *(in press)*.

13. Boudewijns R, Thibaut HJ, Kaptein SJF, Li R, Vergote V, Seldeslachts L, et al. STAT2 signaling as double-edged sword restricting viral dissemination but driving severe pneumonia in SARS-CoV-2 infected hamsters. bioRxiv. 2020.

14. Enkirch T, von Messling V. Ferret models of viral pathogenesis. Virology. 2015;479-480:259-70. Epub 2015/03/31. doi: 10.1016/j.virol.2015.03.017. PubMed PMID: 25816764; PubMed Central PMCID: PMCPMC7111696.

15. Martina BE, Haagmans BL, Kuiken T, Fouchier RA, Rimmelzwaan GF, Van Amerongen G, et al. Virology: SARS virus infection of cats and ferrets. Nature. 2003;425(6961):915. Epub 2003/10/31. doi: 10.1038/425915a. PubMed PMID: 14586458; PubMed Central PMCID: PMCPMC7094990.

16. Kim YI, Kim SG, Kim SM, Kim EH, Park SJ, Yu KM, et al. Infection and Rapid Transmission of SARS-CoV-2 in Ferrets. Cell Host Microbe. 2020. Epub 2020/04/08. doi: 10.1016/j.chom.2020.03.023

10.1016/j.chom.2020.03.023. PubMed PMID: 32259477.

17. Richard M, Kok A, de Meulder D, Bestebroer TM, Lamers MM, Okba NMA, et al. SARS-CoV-2 is transmitted via contact and via the air between ferrets. Nat Commun. 2020;11(1):3496. Epub 2020/07/10. doi: 10.1038/s41467-020-17367-2. PubMed PMID: 32641684; PubMed Central PMCID: PMCPMC7343828.

18. Matute-Bello G, Frevert CW, Martin TR. Animal models of acute lung injury. Am J Physiol Lung Cell Mol Physiol. 2008;295(3):L379-99. Epub 2008/07/16. doi: 10.1152/ajplung.00010.2008. PubMed PMID: 18621912; PubMed Central PMCID: PMCPMC2536793.

19. Estes JD, Wong SW, Brenchley JM. Nonhuman primate models of human viral infections. Nat Rev Immunol. 2018;18(6):390-404. Epub 2018/03/21. doi: 10.1038/s41577-018-0005-7. PubMed PMID: 29556017; PubMed Central PMCID: PMCPMC5970954.

20. Cleary SJ, Pitchford SC, Amison RT, Carrington R, Robaina Cabrera CL, Magnen M, et al. Animal models of mechanisms of SARS-CoV-2 infection and COVID-19 pathology. Br J Pharmacol. 2020. Epub 2020/05/29. doi: 10.1111/bph.15143. PubMed PMID: 32462701; PubMed Central PMCID: PMCPMC7283621.

21. Greenough TC, Carville A, Coderre J, Somasundaran M, Sullivan JL, Luzuriaga K, et al. Pneumonitis and multi-organ system disease in common marmosets (Callithrix jacchus) infected with the severe acute respiratory syndrome-associated coronavirus. Am J Pathol. 2005;167(2):455-63. Epub 2005/07/29. doi: 10.1016/S0002-9440(10)62989-6. PubMed PMID: 16049331; PubMed Central PMCID: PMCPMC1603565.

22. Yu P, Xu Y, Deng W, Bao L, Huang L, Xu Y, et al. Comparative pathology of rhesus macaque and common marmoset animal models with Middle East respiratory syndrome coronavirus. PLoS One. 2017;12(2):e0172093. Epub 2017/02/25. doi: 10.1371/journal.pone.0172093. PubMed PMID: 28234937; PubMed Central PMCID: PMCPMC5325479.

23. Lu S, Zhao Y, Yu W, Yang Y, Gao J, Wang J, et al. Comparison of nonhuman primates identified the suitable model for COVID-19. Signal Transduct Target Ther. 2020;5(1):157. Epub

2020/08/21. doi: 10.1038/s41392-020-00269-6. PubMed PMID: 32814760; PubMed Central PMCID: PMCPMC7434851.

24. Singh A, Singh RS, Sarma P, Batra G, Joshi R, Kaur H, et al. A Comprehensive Review of Animal Models for Coronaviruses: SARS-CoV-2, SARS-CoV, and MERS-CoV. Virol Sin. 2020;35(3):290-304. Epub 2020/07/02. doi: 10.1007/s12250-020-00252-z. PubMed PMID: 32607866; PubMed Central PMCID: PMCPMC7324485.

25. Woolsey C, Borisevich V, Prasad AN, Agans KN, Deer DJ, Dobias NS, et al. Establishment of an African green monkey model for COVID-19. bioRxiv. 2020. Epub 2020/06/09. doi: 10.1101/2020.05.17.100289. PubMed PMID: 32511377; PubMed Central PMCID: PMCPMC7263506.

26. Hartman AL, Nambulli S, McMillen CM, White AG, Tilston-Lunel NL, Albe JR, et al. SARS-CoV-2 infection of African green monkeys results in mild respiratory disease discernible by PET/CT imaging and shedding of infectious virus from both respiratory and gastrointestinal tracts. PLoS Pathog. 2020;16(9):e1008903. Epub 2020/09/19. doi: 10.1371/journal.ppat.1008903. PubMed PMID: 32946524.

27. Gong SR, Bao LL. The battle against SARS and MERS coronaviruses: Reservoirs and Animal Models. Animal Model Exp Med. 2018;1(2):125-33. Epub 2019/03/21. doi: 10.1002/ame2.12017

10.1002/ame2.12017. eCollection 2018 Jun. PubMed PMID: 30891557.

28. Sutton TC, Subbarao K. Development of animal models against emerging coronaviruses: From SARS to MERS coronavirus. Virology. 2015;479-480:247-58. Epub 2015/03/21. doi: 10.1016/j.virol.2015.02.030

10.1016/j.virol.2015.02.030. Epub 2015 Mar 16. PubMed PMID: 25791336.

29. Finch CL, Crozier I, Lee JH, Byrum R, Cooper TK, Liang J, et al. Characteristic and quantifiable COVID-19-like abnormalities in CT- and PET/CT-imaged lungs of SARS-CoV-2-infected crab-eating macaques (Macaca fascicularis). bioRxiv. 2020. Epub 2020/06/09. doi: 10.1101/2020.05.14.096727. PubMed PMID: 32511338; PubMed Central PMCID: PMCPMC7241101.

30. Rockx B, Kuiken T, Herfst S, Bestebroer T, Lamers MM, Oude Munnink BB, et al. Comparative pathogenesis of COVID-19, MERS, and SARS in a nonhuman primate model. Science. 2020;368(6494):1012-5. Epub 2020/04/19. doi: 10.1126/science.abb7314. PubMed PMID: 32303590; PubMed Central PMCID: PMCPMC7164679.

31. Maisonnasse P, Guedj J, Contreras V, Behillil S, Solas C, Marlin R, et al. Hydroxychloroquine use against SARS-CoV-2 infection in non-human primates. Nature. 2020. Epub 2020/07/23. doi: 10.1038/s41586-020-2558-4. PubMed PMID: 32698191.

32. Chandrashekar A, Liu J, Martinot AJ, McMahan K, Mercado NB, Peter L, et al. SARS-CoV-2 infection protects against rechallenge in rhesus macaques. Science. 2020;369(6505):812-7. Epub 2020/05/22. doi: 10.1126/science.abc4776. PubMed PMID: 32434946; PubMed Central PMCID: PMCPMC7243369.

33. Deng W, Bao L, Gao H, Xiang Z, Qu Y, Song Z, et al. Ocular conjunctival inoculation of SARS-CoV-2 can cause mild COVID-19 in rhesus macaques. Nat Commun. 2020;11(1):4400. Epub 2020/09/04. doi: 10.1038/s41467-020-18149-6. PubMed PMID: 32879306.

34. Williamson BN, Feldmann F, Schwarz B, Meade-White K, Porter DP, Schulz J, et al. Clinical benefit of remdesivir in rhesus macaques infected with SARS-CoV-2. Nature. 2020;585(7824):273-6. Epub 2020/06/10. doi: 10.1038/s41586-020-2423-5. PubMed PMID: 32516797; PubMed Central PMCID: PMCPMC7486271.

627 35. van Doremalen N, Lambe T, Spencer A, Belij-Rammerstorfer S, Purushotham JN, Port
628 JR, et al. ChAdOx1 nCoV-19 vaccine prevents SARS-CoV-2 pneumonia in rhesus macaques.
629 Nature. 2020. Epub 2020/07/31. doi: 10.1038/s41586-020-2608-y. PubMed PMID: 32731258.
630 36. Gao Q, Bao L, Mao H, Wang L, Xu K, Yang M, et al. Development of an inactivated
631 vaccine candidate for SARS-CoV-2. Science. 2020;369(6499):77-81. Epub 2020/05/08. doi:
632 10.1126/science.abc1932. PubMed PMID: 32376603; PubMed Central PMCID:
633 PMCPMC7202686.
634 37. Erasmus JH, Khandhar AP, O'Connor MA, Walls AC, Hemann EA, Murapa P, et al. An
635 Alphavirus-derived replicon RNA vaccine induces SARS-CoV-2 neutralizing antibody and T cell
636 responses in mice and nonhuman primates. Sci Transl Med. 2020;12(555). Epub 2020/07/22.
637 doi: 10.1126/scitranslmed.abc9396. PubMed PMID: 32690628; PubMed Central PMCID:
638 PMCPMC7402629.
639 38. Mercado NB, Zahn R, Wegmann F, Loos C, Chandrashekar A, Yu J, et al. Single-shot
640 Ad26 vaccine protects against SARS-CoV-2 in rhesus macaques. Nature. 2020. Epub
641 2020/07/31. doi: 10.1038/s41586-020-2607-z. PubMed PMID: 32731257.
642 39. Yu J, Tostanoski LH, Peter L, Mercado NB, McMahan K, Mahrokhian SH, et al. DNA
643 vaccine protection against SARS-CoV-2 in rhesus macaques. Science. 2020;369(6505):806-11.
644 Epub 2020/05/22. doi: 10.1126/science.abc6284. PubMed PMID: 32434945; PubMed Central
645 PMCID: PMCPMC7243363.
646 40. Patel A, Walters J, Reuschel EL, Schultheis K, Parzych E, Gary EN, et al. Intradermal-
647 delivered DNA vaccine provides anamnestic protection in a rhesus macaque SARS-CoV-2
648 challenge model. bioRxiv. 2020.
649 41. Corbett KS, Flynn B, Foulds KE, Francica JR, Boyoglu-Barnum S, Werner AP, et al.
650 Evaluation of the mRNA-1273 Vaccine against SARS-CoV-2 in Nonhuman Primates. N Engl J
651 Med. 2020. Epub 2020/07/30. doi: 10.1056/NEJMoa2024671. PubMed PMID: 32722908;
652 PubMed Central PMCID: PMCPMC7449230.
653 42. Yang J, Wang W, Chen Z, Lu S, Yang F, Bi Z, et al. A vaccine targeting the RBD of the S
654 protein of SARS-CoV-2 induces protective immunity. Nature. 2020. Epub 2020/07/30. doi:
655 10.1038/s41586-020-2599-8. PubMed PMID: 32726802.
656 43. Hatziioannou T, Ambrose Z, Chung NP, Piatak M, Jr., Yuan F, Trubey CM, et al. A
657 macaque model of HIV-1 infection. Proc Natl Acad Sci U S A. 2009;106(11):4425-9. Epub
658 2009/03/04. doi: 10.1073/pnas.0812587106. PubMed PMID: 19255423; PubMed Central
659 PMCID: PMCPMC2657417.
660 44. Zhou Y, Bao R, Haigwood NL, Persidsky Y, Ho WZ. SIV infection of rhesus macaques of
661 Chinese origin: a suitable model for HIV infection in humans. Retrovirology. 2013;10:89. Epub
662 2013/08/21. doi: 10.1186/1742-4690-10-89. PubMed PMID: 23947613; PubMed Central
663 PMCID: PMCPMC3765527.
664 45. Foreman TW, Mehra S, Lackner AA, Kaushal D. Translational Research in the
665 Nonhuman Primate Model of Tuberculosis. ILAR J. 2017;58(2):151-9. Epub 2017/06/03. doi:
666 10.1093/ilar/ilx015. PubMed PMID: 28575319; PubMed Central PMCID: PMCPMC6279141.
667 46. Cardona PJ, Williams A. Experimental animal modelling for TB vaccine development.
668 Int J Infect Dis. 2017;56:268-73. Epub 2017/02/07. doi: 10.1016/j.ijid.2017.01.030. PubMed
669 PMID: 28163168.
670 47. Mooij P, Koopman G, Mortier D, van Heteren M, Oostermeijer H, Fagrouch Z, et al.
671 Pandemic Swine-Origin H1N1 Influenza Virus Replicates to Higher Levels and Induces More
672 Fever and Acute Inflammatory Cytokines in Cynomolgus versus Rhesus Monkeys and Can
673 Replicate in Common Marmosets. PLoS One. 2015;10(5):e0126132. Epub 2015/05/07. doi:

674 10.1371/journal.pone.0126132. PubMed PMID: 25946071; PubMed Central PMCID:
675 PMCPMC4422689.
676 48. Wang L. C-reactive protein levels in the early stage of COVID-19. Med Mal Infect.
677 2020;50(4):332-4. Epub 2020/04/04. doi: 10.1016/j.medmal.2020.03.007. PubMed PMID:
678 32243911; PubMed Central PMCID: PMCPMC7146693.
679 49. Ronco C, Reis T. Kidney involvement in COVID-19 and rationale for extracorporeal
680 therapies. Nat Rev Nephrol. 2020;16(6):308-10. Epub 2020/04/11. doi: 10.1038/s41581-020-
681 0284-7. PubMed PMID: 32273593; PubMed Central PMCID: PMCPMC7144544.
682 50. Ronco C, Reis T, Husain-Syed F. Management of acute kidney injury in patients with
683 COVID-19. Lancet Respir Med. 2020;8(7):738-42. Epub 2020/05/18. doi: 10.1016/S2213-
684 2600(20)30229-0. PubMed PMID: 32416769; PubMed Central PMCID: PMCPMC7255232.
685 51. Cheng Y, Luo R, Wang K, Zhang M, Wang Z, Dong L, et al. Kidney disease is associated
686 with in-hospital death of patients with COVID-19. Kidney Int. 2020;97(5):829-38. Epub
687 2020/04/06. doi: 10.1016/j.kint.2020.03.005. PubMed PMID: 32247631; PubMed Central
688 PMCID: PMCPMC7110296.
689 52. Spiezia L, Boscolo A, Poletto F, Cerruti L, Tiberio I, Campello E, et al. COVID-19-Related
690 Severe Hypercoagulability in Patients Admitted to Intensive Care Unit for Acute Respiratory
691 Failure. Thromb Haemost. 2020;120(6):998-1000. Epub 2020/04/22. doi: 10.1055/s-0040-
692 1710018. PubMed PMID: 32316063; PubMed Central PMCID: PMCPMC7295272.
693 53. Connors JM, Levy JH. COVID-19 and its implications for thrombosis and
694 anticoagulation. Blood. 2020;135(23):2033-40. Epub 2020/04/28. doi:
695 10.1182/blood.2020006000. PubMed PMID: 32339221; PubMed Central PMCID:
696 PMCPMC7273827.
697 54. Munster VJ, Feldmann F, Williamson BN, van Doremalen N, Perez-Perez L, Schulz J, et
698 al. Respiratory disease in rhesus macaques inoculated with SARS-CoV-2. Nature.
699 2020;585(7824):268-72. Epub 2020/05/13. doi: 10.1038/s41586-020-2324-7. PubMed PMID:
700 32396922; PubMed Central PMCID: PMCPMC7486227.
701 55. Coperchini F, Chiovato L, Croce L, Magri F, Rotondi M. The cytokine storm in COVID-
702 19: An overview of the involvement of the chemokine/chemokine-receptor system. Cytokine
703 Growth Factor Rev. 2020;53:25-32. Epub 2020/05/25. doi: 10.1016/j.cytogfr.2020.05.003.
704 PubMed PMID: 32446778; PubMed Central PMCID: PMCPMC7211650.
705 56. Huang C, Wang Y, Li X, Ren L, Zhao J, Hu Y, et al. Clinical features of patients infected
706 with 2019 novel coronavirus in Wuhan, China. Lancet. 2020;395(10223):497-506. Epub
707 2020/01/28. doi: 10.1016/S0140-6736(20)30183-5. PubMed PMID: 31986264; PubMed
708 Central PMCID: PMCPMC7159299.
709 57. Hope MD, Raptis CA, Shah A, Hammer MM, Henry TS, six s. A role for CT in COVID-19?
710 What data really tell us so far. Lancet. 2020;395(10231):1189-90. Epub 2020/04/01. doi:
711 10.1016/S0140-6736(20)30728-5. PubMed PMID: 32224299; PubMed Central PMCID:
712 PMCPMC7195087.
713 58. Simpson S, Kay FU, Abbara S, Bhalla S, Chung JH, Chung M, et al. Radiological Society
714 of North America Expert Consensus Statement on Reporting Chest CT Findings Related to
715 COVID-19. Endorsed by the Society of Thoracic Radiology, the American College of Radiology,
716 and RSNA - Secondary Publication. J Thorac Imaging. 2020;35(4):219-27. Epub 2020/04/24.
717 doi: 10.1097/RTI.0000000000000524. PubMed PMID: 32324653; PubMed Central PMCID:
718 PMCPMC7255403.
719 59. Fan L, Liu S. CT and COVID-19: Chinese experience and recommendations concerning
720 detection, staging and follow-up. Eur Radiol. 2020;30(9):5214-6. Epub 2020/05/08. doi:

721 10.1007/s00330-020-06898-3. PubMed PMID: 32377812; PubMed Central PMCID:
722 PMCPMC7202679.
723 60. Brining DL, Mattoon JS, Kercher L, LaCasse RA, Safronetz D, Feldmann H, et al. Thoracic
724 radiography as a refinement methodology for the study of H1N1 influenza in cynomologus
725 macaques (Macaca fascicularis). Comp Med. 2010;60(5):389-95. Epub 2011/01/26. PubMed
726 PMID: 21262125; PubMed Central PMCID: PMCPMC2958208.
727 61. Corman VM, Landt O, Kaiser M, Molenkamp R, Meijer A, Chu DK, et al. Detection of
728 2019 novel coronavirus (2019-nCoV) by real-time RT-PCR. Euro Surveill. 2020;25(3). Epub
729 2020/01/30. doi: 10.2807/1560-7917.ES.2020.25.3.2000045. PubMed PMID: 31992387;
730 PubMed Central PMCID: PMCPMC6988269.
731 62. Pan F, Ye T, Sun P, Gui S, Liang B, Li L, et al. Time Course of Lung Changes at Chest CT
732 during Recovery from Coronavirus Disease 2019 (COVID-19). Radiology. 2020;295(3):715-21.
733 Epub 2020/02/14. doi: 10.1148/radiol.2020200370. PubMed PMID: 32053470; PubMed
734 Central PMCID: PMCPMC7233367.
735 63. Hoste ACR, Venteo A, Fresco-Taboada A, Tapia I, Monedero A, Lopez L, et al. Two
736 serological approaches for detection of antibodies to SARS-CoV-2 in different scenarios: a
737 screening tool and a point-of-care test. Diagn Microbiol Infect Dis. 2020;98(4):115167. Epub
738 2020/09/06. doi: 10.1016/j.diagmicrobio.2020.115167. PubMed PMID: 32890908; PubMed
739 Central PMCID: PMCPMC7417941.
740

741

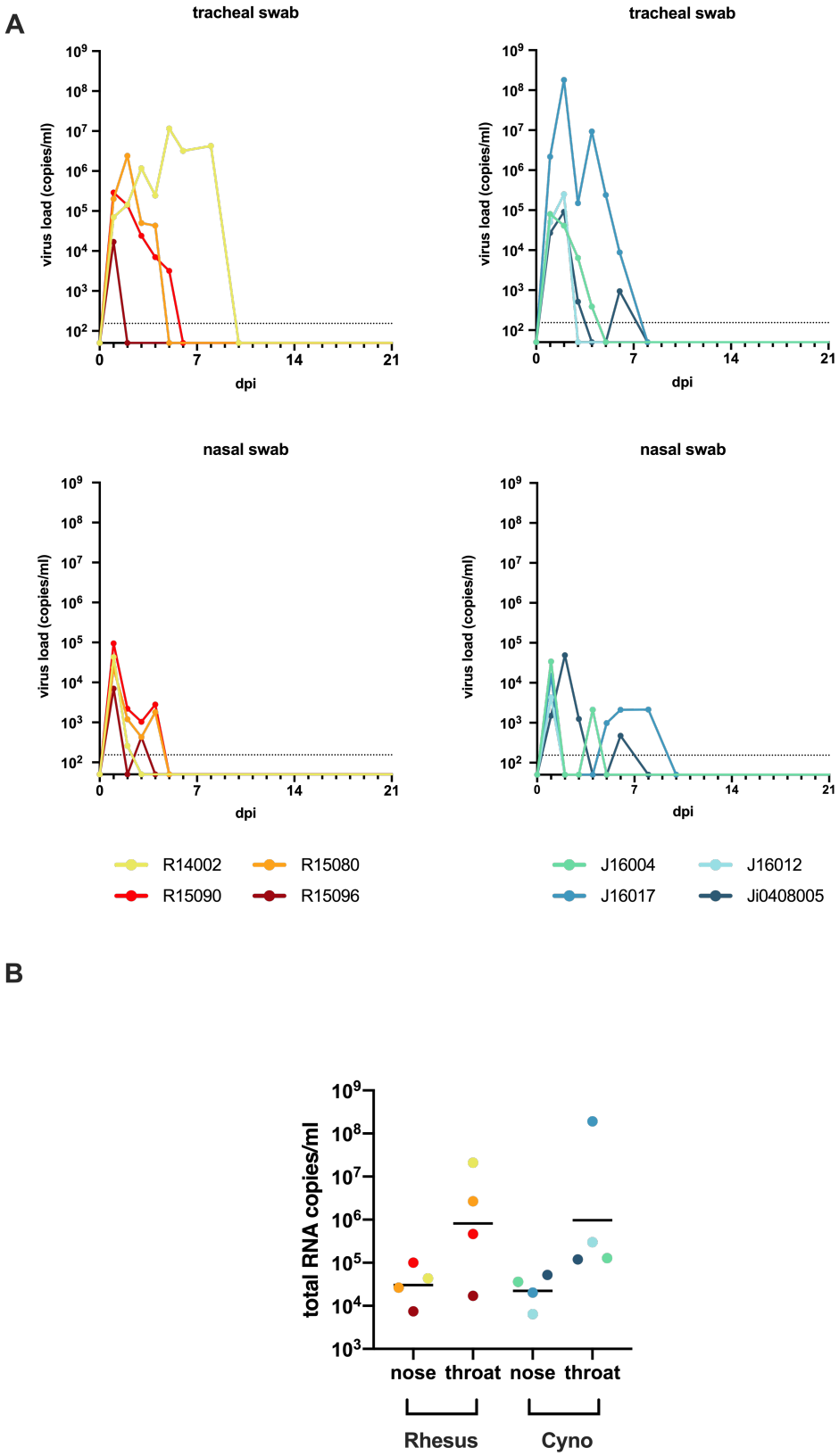

742

743 **Fig 1. Virus load in swab samples.** (A) Viral RNA quantification in tracheal and nasal swabs of

744 rhesus and cynomolgus macaques by qRT-PCR. The limit of quantification (154 RNA

745 copies/ml) is indicated by the dotted horizontal line. (B) Total virus loads in throat and nose
746 samples of macaques throughout the study. Horizontal bars represent geometric means. The
747 sum of the viral copies was calculated rather than area under the curve (AUC), as AUC
748 interpolates for time points when virus loads were not determined.
749 The different colors used for each animal as shown in the legend of 1A are used to denote
750 the same individual in all figures of this manuscript. The group of rhesus macaques is
751 indicated by yellow to red colors; cynomolgus macaques by green to blue. In each graph
752 rhesus macaques are depicted left and cynomolgus macaques right.
753

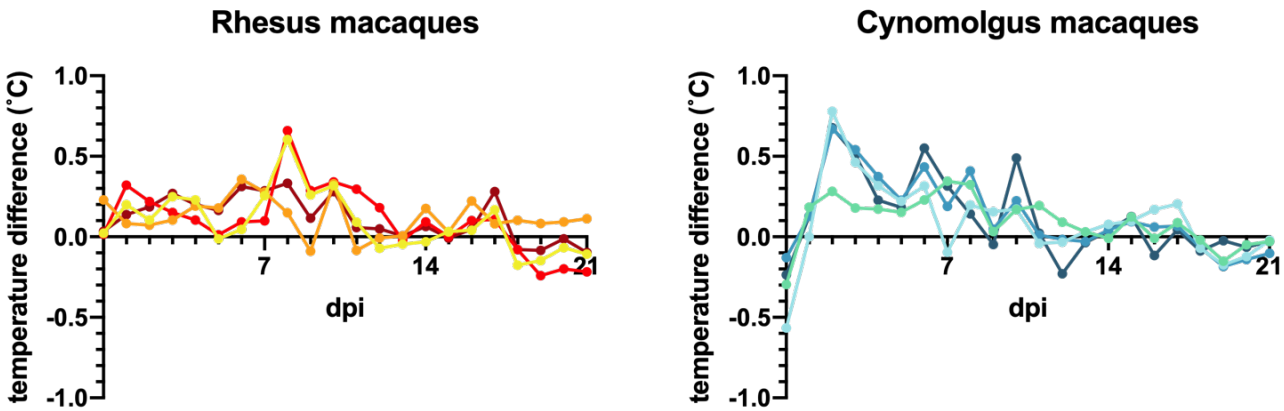

754

755 **Fig 2. Body temperature during the study**. The body temperature was measured by
756 telemetry throughout the study. The daily average body temperature of rhesus and
757 cynomolgus macaques was calculated and the deviations from baseline body temperature
758 (in °C) are depicted. Measurements done during biotechnical handlings were omitted from
759 the calculations.
760

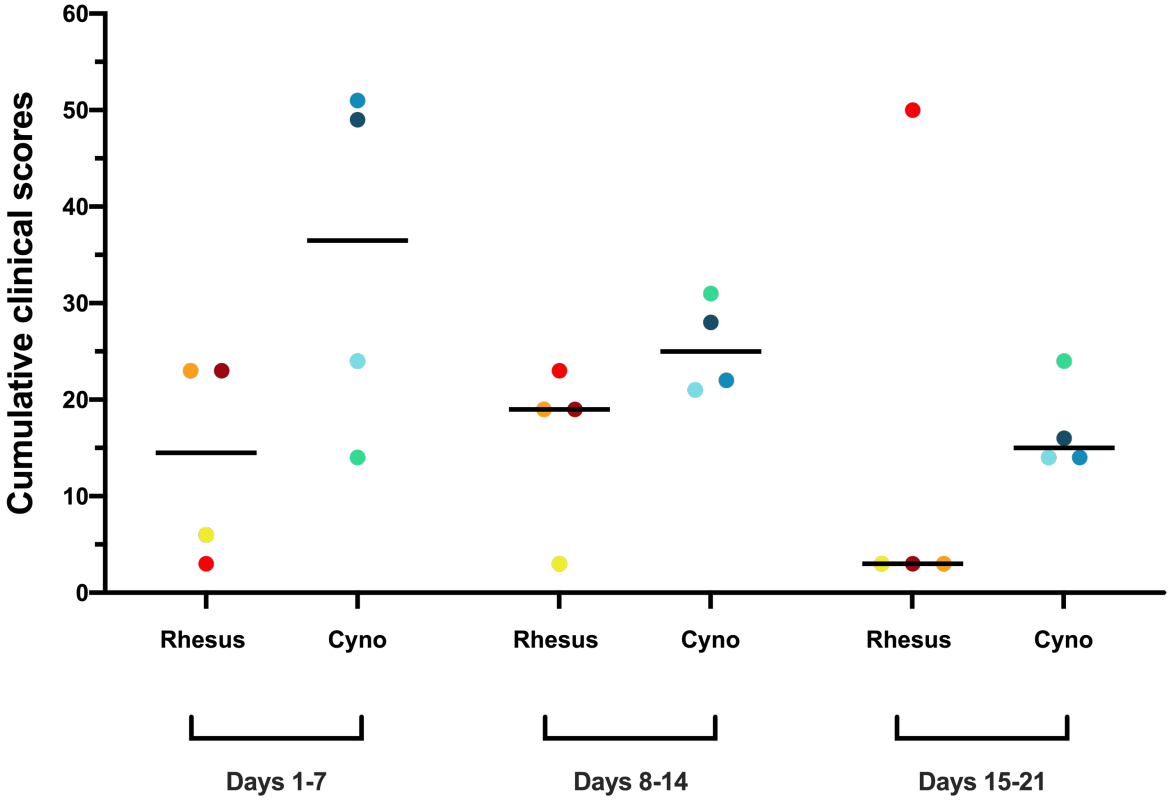

761

762 **Fig 3. Cumulative clinical scores.** The cumulative clinical scores were calculated per week

763 and per individual animal (day 1-7, 8-14 and 15-21). Horizontal bars represent medians.

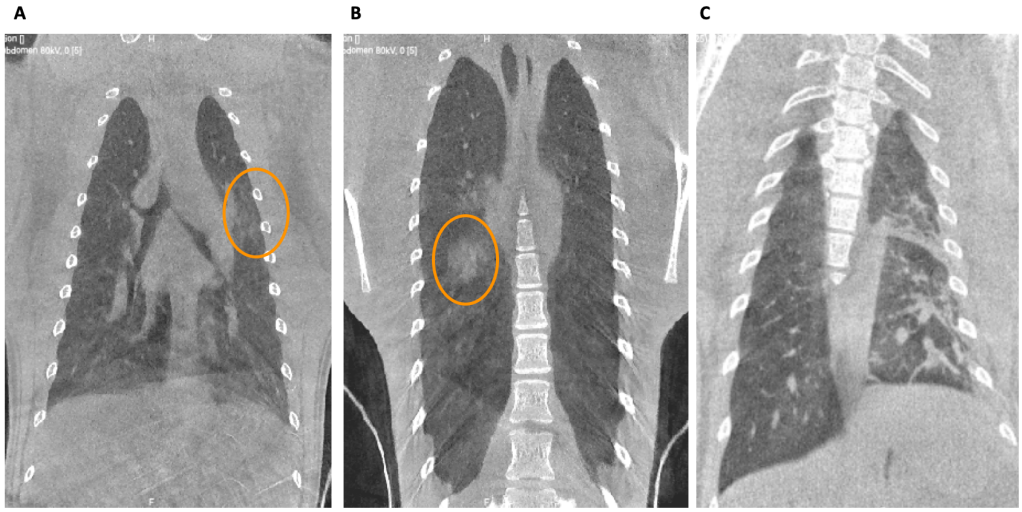

764

765 **Fig 4. Types of lung lesions detected via CT scans in SARS-CoV-2-infected macaques. (**A)

766 Ground glass opacities (GGO), (B) consolidations, and (C) crazy paving patterns (CCP).

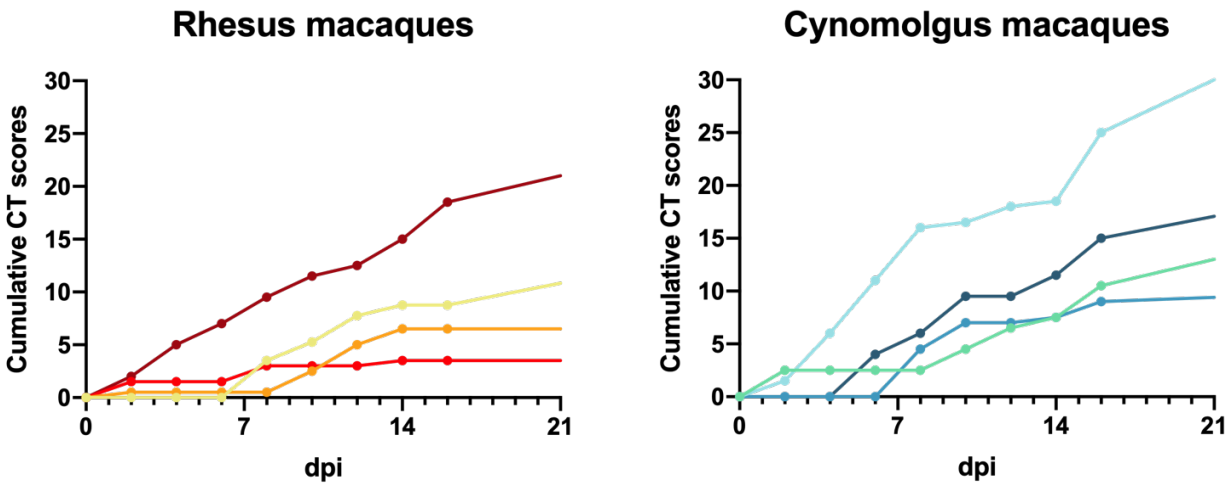

767

768 **Fig 5. Cumulative CT scores.** Cumulative CT scores for each animal were calculated based on

769 the CT scores depicted in Table 1.

770

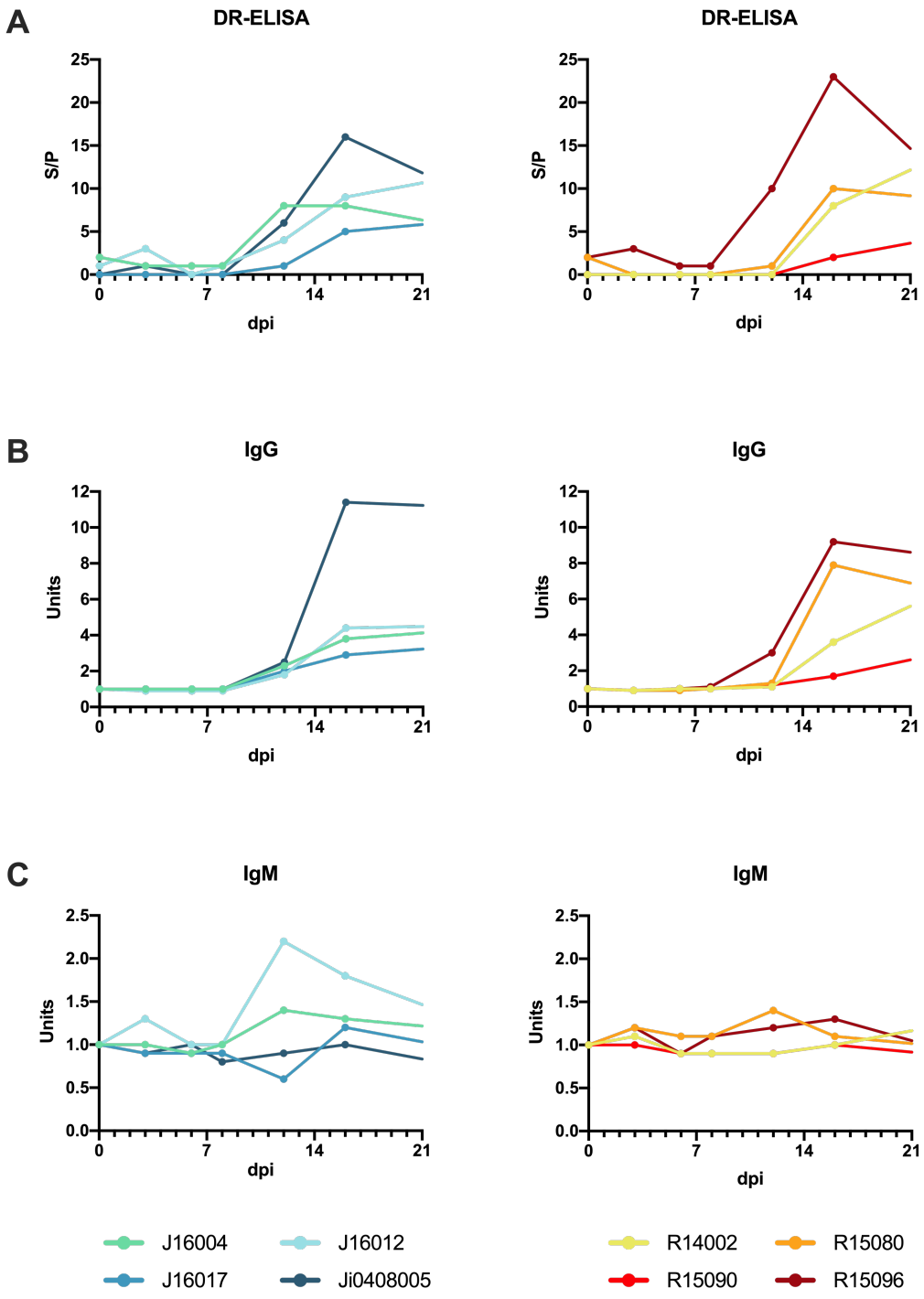

771

772 **Fig 6. Development of SARS-CoV-2 antibody response in rhesus and cynomolgus**

773 **macaques.** The humoral immune response was determined using (A) DR-ELISA measuring

774 the total antibody response, (B) an IgG-specific IgG assay, and (C) an IgM-specific IgM

775 serological test. Results are shown as S/P: sample to positive control ratio:

776 $S/P = \frac{test\ sample - mean\ negative\ control}{mean\ positive\ control - mean\ negative\ control}$ and $Units = \frac{test\ sample\ at\ x\ dpi}{test\ sample\ at\ 0\ dpi}$.